INFECTION AND IMMUNITY, Sept. 2009, p. 3596–3601 Vol. 77, No. 9
0019-9567/09/$08.00+0 doi:10.1128/IAI.00186-09

Injection of *Staphylococcus aureus* EDIN by the *Bacillus anthracis* Protective Antigen Machinery Induces Vascular Permeability▽†

Monica Rolando,[1,2] Patrick Munro,[1,2] Caroline Stefani,[1,2] Patrick Auberger,[1,2,3] Gilles Flatau,[1,2] and Emmanuel Lemichez[1,2,4]*

INSERM, U895, Equipe 6, C3M, Microbial Toxins in Host Pathogen Interactions, Nice F-06204, France[1]; Université de Nice-Sophia-Antipolis, UFR Médecine, IFR50, Nice F-06204, France[2]; INSERM, U895, Equipe 2, C3M, Mort cellulaire, differentiation et cancer, Nice F-06107, France[3]; and Centre Hospitalier Universitaire de Nice, Hôpital l'Archet, Laboratoire de Bactériologie, Nice F-06204, France[4]

Received 18 February 2009/Returned for modification 8 April 2009/Accepted 28 May 2009

Systemic injection of *Bacillus anthracis* lethal toxin (LT) produces vascular leakage and animal death. Recent studies suggest that LT triggers direct endothelial cell cytotoxicity that is responsible for the vascular leakage. LT is composed of heptamers of protective antigen (PA), which drives the endocytosis and translocation into host cells of the lethal factor (LF), a mitogen-activated protein kinase kinase protease. Here we investigated the consequences of injection of an endothelium-permeabilizing factor using LT as a "molecular syringe." To this end, we generated the chimeric factor LE, corresponding to the PA-binding domain of LF (LF_{1-254}) fused to EDIN exoenzyme. EDIN ADP ribosylates RhoA, leading to actin cable disruption and formation of transcellular tunnels in endothelial cells. We report that systemic injection of LET (LE plus PA) triggers a PA-dependent increase in the pulmonary endothelium permeability. We also report that native LT induces a progressive loss of endothelium barrier function. We established that there is a direct correlation between the extent of endothelium permeability induced by LT and the cytotoxic activity of LT. This suggests new ways to design therapeutic drugs against anthrax directed toward vascular permeability.

Bacillus anthracis, the systemic agent of anthrax disease, is a gram-positive bacterial pathogen of humans and animals. It produces a toxin composed of three polypeptides, the edema factor (EF), the lethal factor (LF), and the protective antigen (PA). EF and LF have adenylate cyclase and mitogen-activated protein (MAP) kinase kinase-metalloprotease enzymatic activities, respectively. PA binds a cellular receptor and forms heptamers, allowing endocytosis and translocation of EF and/or LF into the cell cytosol in an AB_7-type toxin model (1, 4, 10). Two von Willebrand factor A-like domain-containing receptors for PA have been characterized: tumor endothelial marker 8 and capillary morphogenesis protein 2 (8, 23). Tumor endothelial marker 8 is highly expressed in epithelial cells lining *B. anthracis* entry sites and tumor vasculature, whereas capillary morphogenesis protein 2 is expressed in most human cells (6, 22). Lethal toxin (LT) (PA plus LF) and the toxin ET (PA plus EF) have different effects during *B. anthracis*-induced animal death. Consistently, deletion of EF and deletion of LF lead to 10- and 1,000-fold attenuation of the bacterial virulence, respectively (21).

Vascular lesions have been identified as a basis for prominent hemorrhages in human pulmonary anthrax, and it is now clear that necrosis of arteries and veins is the most likely source of large hemorrhages in tissues (15). In a primate model, the lung was shown to be the primary target organ. The outcomes of infection included changes in vascular permeability, serosanguinous pleural effusions, and intraalveolar edema (25). Recent studies with mice and rats confirmed that there is LT-mediated, cytokine-independent vascular leakage (19, 20).

Moreover, a direct effect of LT on induction of leakage from vessels was reported for an intradermal intoxication model in mice (14). This effect could be related to direct endothelial cell targeting of LT that triggers direct cytotoxic effects on the endothelial cell actin cytoskeleton and/or viability (17, 26). An in vivo zebrafish model has recently been developed, which allows imaging of the vasculature and of the cardiovascular function of the embryo. The authors showed that there was an increase in endothelial permeability with very little cell death throughout LT-inoculated embryos (5). This suggests that LT has a major role in corrupting the actin cytoskeleton organization when the endothelium barrier function is compromised. The RhoA GTPase regulates the formation and contractility of cellular actin cables and thus also controls the formation of intercellular gaps and endothelium permeability (27). On the other hand, robust inhibition of RhoA and disruption of cytosolic actin filaments by bacterial RhoA ADP ribosylation enzymes, such as EDIN of *Staphylococcus aureus*, lead to opening of transcellular tunnels called macroapertures (7). The opening of macroapertures increases endothelium permeability without disrupting intercellular junctions or inducing cell death (7).

Here we used a PA vectorization system of EDIN. This system corresponds to an LE chimeric factor, LF_{1-254}-EDIN, made by fusing the PA-binding domain of LF (LF_{1-254}) to EDIN exoenzyme. We verified that both LF and LE enter cells in a PA-dependent manner. In addition, we observed that LT

* Corresponding author. Mailing address: Bâtiment Universitaire Archimed, INSERM, U895, Equipe 6, C3M, 151 Route de Saint Antoine de Ginestière, BP 2 3194, F-06204 Nice Cedex 3, France. Phone: 00 33 (0)4 89 06 42 63. Fax: 00 33 (0)4 89 06 42 60. E-mail: lemichez@unice.fr.

† Supplemental material for this article may be found at http://iai.asm.org/.

▽ Published ahead of print on 22 June 2009.

and LET (LE plus PA) cleaved MAP kinase kinase and inactivated RhoA, respectively, with the same kinetics. We show here that, although LET disrupts actin cables, in contrast to LT, which induces the formation of thick actin cables, both toxins lead to an increase in endothelium permeability. This finding also provides evidence that there is a direct correlation between the extent of endothelium permeability and the catalytic activity of LT.

MATERIALS AND METHODS

Cell culture and reagents. Human umbilical vein endothelial cells (HUVECs) (PromoCell) were cultured in human endothelial serum-free medium supplemented with 20% fetal bovine serum, 20 ng/ml basic fibroblast growth factor, 10 ng/ml epidermal growth factor (Invitrogen), and 1 μg/ml heparin (Sigma). Cell transfection with the green fluorescent protein-actin expression construct has been described previously (7).

Monoclonal anti-CD31 antibody (clone MEC13.3) was purchased from BD Pharmingen; anti-RhoA (clone 26C4) and anti-cadherin 5 (clone 75) were purchased from BD Biosciences; rabbit anti-MEK2-N20 was purchased from Santa Cruz Technologies; and rabbit anti-p-$ERK_{1/2}$ and anti-$ERK_{1/2}$ were purchased from Cell Signaling. For immunofluorescence analysis primary antibodies were visualized using Texas Red-conjugated anti-mouse antibodies (Vector; Biovalley) and Texas Red-conjugated anti-rabbit and anti-rat antibodies (Jackson Immunoresearch Laboratories). For immunoblotting, primary antibodies were visualized using goat anti-mouse or anti-rabbit horseradish peroxidase-conjugated secondary antibodies (Dako), followed by ECL chemiluminescence detection (Amersham). All biochemical reagents were purchased from Sigma Aldrich, except staurosporin, which was purchased from MP Biomedicals.

Recombinant toxin production. The PA-encoding gene was cloned with BamHI-SacI into pET22 (Novagen) after PCR amplification using primers 5′-GGATCCCGAATTAAACAGGAGAACCGG and 5′-GAGCTCTGTCCTATCTCATAGCCTTTTTTAGA. The LF-encoding gene was cloned with BamHI-SacI into the pQE30 (Qiagen) expression vector after PCR amplification using primers 5′-GGATCCATGGCGGGCGGTCATGGTGAT and 5′-GAGCTCTTATGAGTTAATAATGAACTTAAT. Genomic DNA of *B. anthracis* Sterne (kindly provided by P. Boquet) was used as the template. An LE (LE_{1-254}EDIN) expression plasmid was constructed by cloning the sequence encoding LF_{1-254} that was NheI-BamHI amplified using oligonucleotides 5′-GCTAGCGCGGGCGGTCATGGTGATGTA and 5′-GGATCCTAGATTTATTTCTTGTTCGTT into the pET28 vector containing EDIN BamHI-EcoRI sites (7). Catalytically inactive mutants LEm (LF_{1-254}-$EDIN_{R185E}$) and LFm (LF_{E687A}) were obtained by using a QuikChange site-directed mutagenesis kit (Stratagene) (7). Plasmids were transformed into *Escherichia coli* BL21(DE3). PA was prepared from the periplasm using a standard protocol. Clarified supernatants containing the various polypeptides were loaded on a nickel column (Amersham Bioscience). Polypeptides were eluted with a step gradient of imidazole. Fractions of polypeptides were pooled and dialyzed overnight against 25 mM Tris-HCl (pH 7.4), 50 mM NaCl. LF, LE, and mutant molecules were further purified with MonoQ columns (Amersham) using a gradient consisting of 25 mM Tris-HCl (pH 7.5) and 50 to 300 mM NaCl. PA was purified with a Q Sepharose fast-flow column (Amersham) with a gradient consisting of 0 to 300 mM NaCl and 20 mM HEPES (pH 7), sieved onto a BioSep-Sec-S column (Phenomenex), and finally purified with a Resource Q column (Amersham) using a gradient consisting of 0 to 300 mM NaCl and 20 mM HEPES (pH 7). Proteins were finally applied to an EndoTrap Red column (Cambrex) to remove lipopolysaccharide, and the absence of detectable amounts of lipopolysaccharide was assessed using *Limulus* amebocyte lysate QCL-1000 (Cambrex).

Rho activity measurement. The amount of active RhoA present in lysates of HUVEC monolayers was determined by affinity chromatography, as previously described (11). Proteins were resolved by 12% sodium dodecyl sulfate-polyacrylamide gel electrophoresis using standard conditions.

In vivo permeability assays. In vivo effects of LT and LET were determined with 6-week-old female BALB/c mice (Janvier, France). Groups of mice were inoculated in the tail vein sequentially with combinations of 50 μg of PA and LF, LFm, LE, or LEm or with 1 μg of EDIN in phosphate-buffered saline (PBS) or PBS alone (control). For a quantitative lung vascular permeability assay, 30 min prior to measurement, intoxicated mice were inoculated in the tail vein with 100 μl of 0.5 g/liter of the molecular tracer fluorescein isothiocyanate-dextran (FITC-dextran, 70,000 molecular weight; Invitrogen) in PBS. Mice were euthanized, and the lungs were washed twice with 0.5 ml of PBS. Bronchoalveolar lavage fluids were recovered, evaporated using Speed Vac concentrator (Savant Instruments, Inc.), and resuspended in 200 μl of sterile water for measurement of fluorescence at 485 and 538 nm, using FlupstarOptima (BMG-Labtech). Values were compared to a standard to estimate quantities of FITC-dextran. The animals used during this study were maintained and handled using standard ethical guidelines (European Union guidelines on animal laboratory care), and experiments were approved by the ethics committee of the Nice School of Medicine. Visualization of lung vascular permeability was performed as described previously (28). Briefly, FITC-dextran was injected into the tail vein. After 30 min mice were euthanized, and lungs were frozen in OCT embedding medium and sectioned with a Thermo-Shandon AS620SME cryostat. Sections (4 μm) were fixed with acetone and stained with monoclonal anti-CD31 (clone MEC13.3) antibody. Slides were examined with an LSM510-Meta confocal microscope (Carl Zeiss). Vascular permeability was evaluated by determining the extent of FITC-dextran diffusion (green label) from the vasculature.

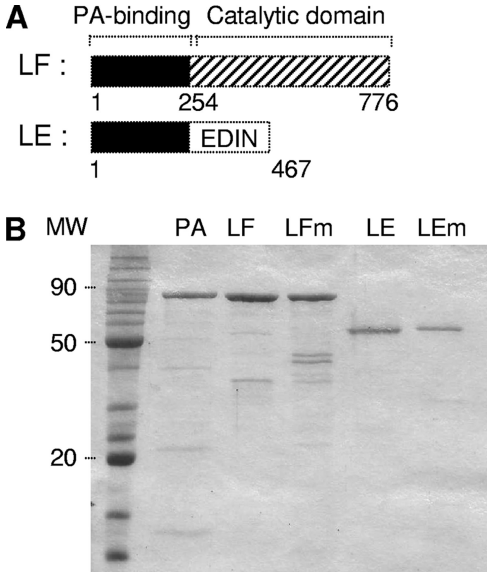

FIG. 1. LE chimera construct. (A) Schematic diagrams of LF of *B. anthracis* and chimeric toxin LE made by swapping the catalytic domain of LF with EDIN of *S. aureus*. (B) Sodium dodecyl sulfate-polyacrylamide gel electrophoresis of recombinant toxins in *E. coli* BL21(DE3). Lane MW, 10- to 120-kDa prestained protein markers (Fermentas).

Immunofluorescence and video microscopy. Immunofluorescence studies were performed using cells fixed in 4% paraformaldehyde (Sigma) in PBS. Actin filaments were labeled using 1 μg/ml FITC-conjugated phalloidin (Sigma). Immunosignals were analyzed with an LSM510-Meta confocal microscope (Carl Zeiss) with a ×63 lens. Each picture represents the projection of six serial confocal sections. Cells were analyzed by video microscopy using an Axiovert 200 microscope equipped with shutter-controlled illumination (Carl Zeiss) and a cooled, digital charge-coupled device camera (Roper Scientific). Images were processed using MetaMorph 2.0 image analysis software (Molecular Devices) and QuickTime pro 7 software (Apple).

Measurement of caspase-3 activity and cell death. HUVECs were intoxicated with LET or staurosporin, and measurements for each condition were obtained in triplicate. Caspase activity was measured at various time points at 37°C in 96-well plates using 35 μg of protein together with 0.5 mM Ac-DEVD-AMC (caspase-3 substrate) (Alexis Biomedicals) in the presence or absence of 10 μM Ac-DEVD-CHO (caspase-3) in order to measure caspase specific activity (Alexis Biomedicals). Measurements were obtained using an Ascent Fluoroskan (Thermo Labsystem). The caspase specific activity was expressed in arbitrary units per mg of protein. For early apoptotic cell determination HUVEC monolayers at passage 3 were simultaneously stained with phycoerythrin-annexin V and 7-amino-actinomycin D (BD Biosciences). The concentrations of the cell suspensions were adjusted to 10^5 cells/ml before acquisition, and the preparations were analyzed with a fluorescence-activated cell sorting flow cytometer (FACSCalibur; BD Biosciences). Data acquisition was performed with the CellQuest software (BD Biosciences).

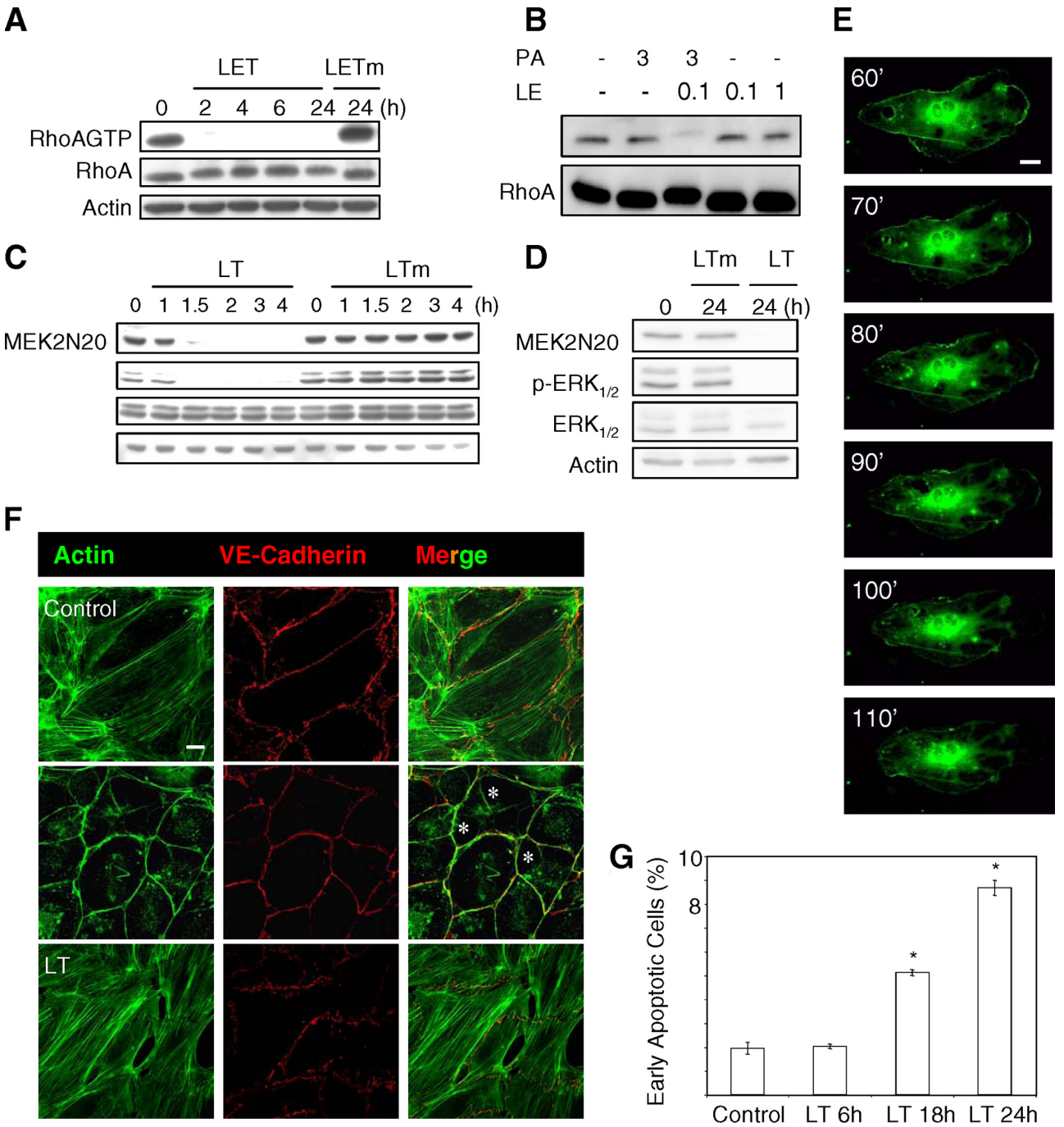

FIG. 2. PA-dependent delivery of LE chimera into endothelial cells. HUVEC monolayers were intoxicated with LET (3 μg/ml PA plus 1 μg/ml LF_{1-254}-EDIN), LETm (3 μg/ml PA plus 1 μg/ml LF_{1-254}-$EDIN_{R185E}$), LT (3 μg/ml PA plus 1 μg/ml LF), or LTm (3 μg/ml PA plus 1 μg/ml LF_{E687A}) for the indicated periods of time. (A and B) The levels of active RhoA (labeled RhoA-GTP) were determined by using glutathione *S*-transferase-Rhotekin receptor-binding domain pull down. The cellular level of RhoA was determined by anti-RhoA immunoblotting of total protein extracts. The Western blot of anti-RhoA and/or anti-actin shows equal protein loading. (C and D) HUVEC monolayers were intoxicated, and the effect of LF was assessed by anti-MEK2N20 and anti-phospho-$ERK_{1/2}$ immunoblotting. The Western blot of anti-actin and anti-$ERK_{1/2}$ shows equal protein loading. (E) Formation of macroapertures in HUVEC monolayers transfected with green fluorescent protein-actin and treated with LET (images from Video S1 in the supplemental material; intervals in minutes). (F) Actin cytoskeleton organization in control or intoxicated monolayers for 2 h with LET or for 24 h with LT. F-actin was labeled with FITC-phalloidin (green), and VE-cadherin adhesion molecules were labeled with anti-cadherin 5 (red). The asterisks indicate LET-induced macroapertures. Scale bar, 10 μm. (G) Effect of LT on endothelial cell apoptosis. Cells were treated with medium alone or with medium supplemented with LT. The bars and error bars indicate the means ± standard deviations of the percentages of early apoptotic cells (phycoerythrin-annexin V positive and 7-amino-actinomycin D negative) for three independent experiments. Statistical data analysis was performed with unpaired two-tailed *t* tests (*, $P < 0.01$ compared with control cells).

RESULTS AND DISCUSSION

PA-vectorized EDIN. No direct correlation has been established between the extent of endothelium permeabilization by LT and the cytotoxic activity of LT. We developed a strategy aimed at testing whether PA vectorization of an endothelium-permeabilizing factor might trigger an increase in the vascular permeability. For this, we used the RhoA-inactivating factor EDIN of *S. aureus*. Previous studies have established that a low level of inhibition of the GTPase RhoA leads to cell spreading and consequently results in stimulation of cell-cell adherence junctions, thus enhancing the monolayer barrier function (9). In contrast, a higher level of inhibition of RhoA results in a decrease in the endothelial barrier function due to the formation of large transcellular tunnels, called macroapertures (7).

In contrast to EDIN, which enters host cells inefficiently by nonspecific macropinocytosis, PA heptamers, by binding the amino-terminal domain of LF (amino acids 1 to 254), can promote efficient endocytosis and intracytoplasmic delivery of heterologous polypeptides fused to LF_{1-254} in the host cell cytosol (1, 3). Hence, the (PA) vectorization system has been exploited to deliver to the cytosol heterologous polypeptides, such as catalytic domains of Shiga and diphtheria toxins (3), cholera toxin (24), and viral particles, such as the envelope glycoprotein of human immunodeficiency virus type 1 (gp120) (13). In order to efficiently transfer EDIN into the cell, we took advantage of these findings to construct a chimeric toxin by swapping the catalytic domain of LF with EDIN (designated LE). LE corresponds to the PA-binding domain of LF (LF_{1-254}) fused to EDIN (Fig. 1A). A catalytically inactive mutant of LE (designated LEm) was obtained by mutagenesis of arginine 185 of EDIN in glutamine, as described previously for arginine 186 of the C3 exoenzyme (18). These factors were then purified as described in Materials and Methods (Fig. 1B).

Functional analysis of PA vectorization of LE. We first characterized the cytotoxic properties of LET. We observed that LET induced inactivation of RhoA with a half-life of <2 h, unlike the catalytically inactive mutant LETm (PA plus LE_{R185E}) (Fig. 2A) or LE alone (Fig. 2B). *B. anthracis* LT induces cell toxicity by cleavage of MEKs, leading to inactivation of MAP kinase signaling pathways (12). We found that LT triggered cleavage of MEK2 and inactivation of $ERK_{1/2}$ with a half-life of <2 h, similar to the kinetics of RhoA inactivation by LET (Fig. 2C). We verified that there was sustained inactivation of MAP kinase signaling for 24 h of intoxication and that LTm, a catalytically inactive mutant of LT, had no effect (Fig. 2C and 2D). Together, these findings show that LF and LE enter cells in a PA-dependent manner. In addition, we found that LT and LET cleaved MAP kinase kinase and inactivated RhoA with the same kinetics, respectively. Our results also show that injection of LE by PA vectorization is remarkably efficient, considering that we previously found that 24 h of intoxication with high doses of the EDIN exoenzyme was required to trigger a 50% decrease in the level of active RhoA (7). Consistent with this, when assessing the biological effect of LET on endothelial monolayers, we observed that cells started to form macroapertures after 1 h of intoxication (Fig. 2E; see Video S1 in the supplemental material). After 2 h, we observed massive formation of macroapertures (Fig. 2F). In addition, after 4 h of intoxication, apertures more than 100 μm in diameter formed as a consequence of the absence of closure, which resulted from the complete inhibition of RhoA (see Video S2 in the supplemental material). No effect on the endothelium was observed upon treatment with either LET_{R185E} or LE alone (not shown). Collectively, these results show that, in contrast to the effect of EDIN alone, PA-dependent internalization of LE results in rapid and complete inactivation of RhoA, leading to the formation of giant apertures in endothelial cells, thus compromising endothelium barrier integrity.

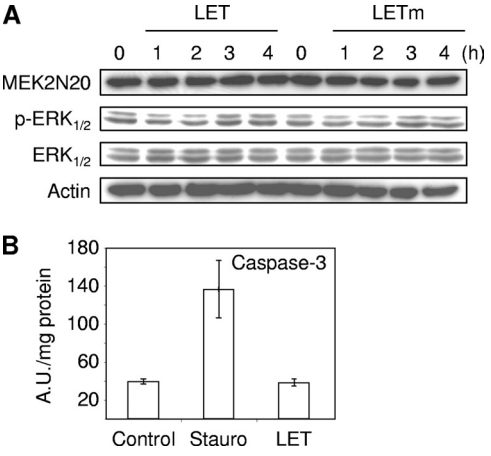

FIG. 3. Molecular activity of LF-EDIN chimera. (A) HUVEC monolayers were intoxicated with LET (3 μg/ml PA plus 1 μg/ml LF_{1-254}-EDIN) or LETm (3 μg/ml LET_{R185E}-PA plus 1 μg/ml LF_{1-254}-$EDIN_{R185E}$) for the indicated periods of time. Immunoblots of anti-MEK2N20, anti-actin, anti-phosphorylated-ERK1/2 (p-$ERK_{1/2}$), and anti-$ERK_{1/2}$ show the absence of activity of LET with $ERK_{1/2}$. (B) Absence of activation of caspase-3 by LET. HUVEC monolayers were intoxicated for 8 h with LET (3 μg/ml PA plus 1 μg/ml LF_{1-254}-EDIN). Staurosporin 1 μM (Stauro) was added as a positive control. The activities are expressed in arbitrary units (A.U.) per mg of proteins (means ± standard deviations of two experiments performed in triplicate).

Recent studies indicated that LT plays a direct role in compromising endothelial barrier function, leading to animal death (5, 17, 26). Initially, LT was reported to trigger endothelial cell death (17). This effect of LT could be observed with both HUVEC and dermal microvascular endothelial cells derived from large vessels and microvessels, respectively (26). In addition, LT was shown to trigger the formation of actin cables and associated intercellular junction disassembly, which were responsible for the increase in endothelium permeability (26). In line with this, LT was found to trigger massive formation of actin cables associated with disruption of intercellular junctions, as well as a belated increase in cell death (Fig. 2F and 2G), as described previously (17, 26). No effects on the actin cytoskeleton were observed with LTm or LF alone (not shown).

We next investigated the effect of PA-vectorized LF_{1-254}-EDIN (LET) on cell signaling pathways corrupted by LT. We observed that LET neither cleaved MEK2 nor inhibited $ERK_{1/2}$ phosphorylation (Fig. 3A). With our system of PA-vectorized LF_{1-254}-EDIN we did not observe activation of caspase-3 with LET (Fig. 3B).

In conclusion, we show that 24 h of intoxication of endothelial cells with LT induces the formation of actin cables and cell

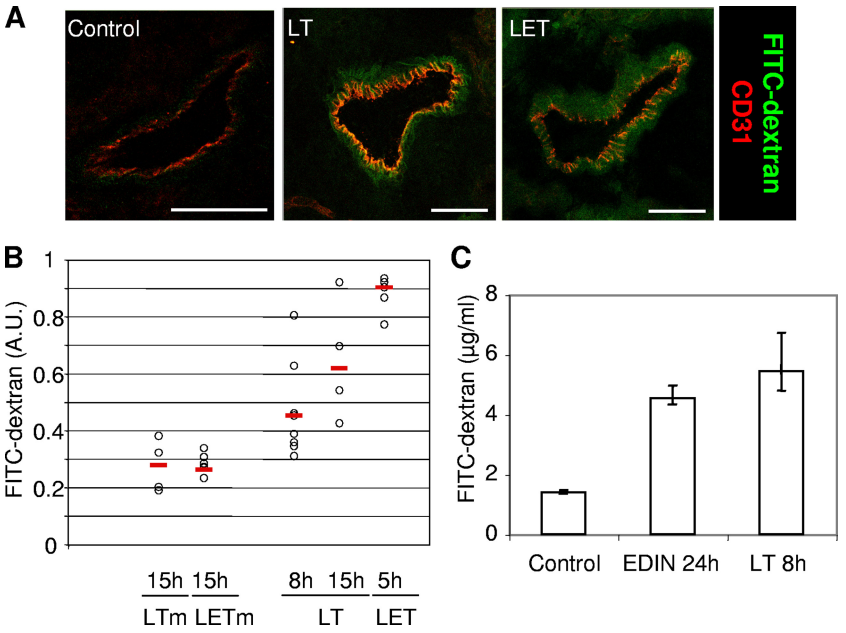

FIG. 4. LET-induced permeability in animals. Mice were inoculated intravenously with LT (100 μg PA plus 100 μg LF), LTm (100 μg PA plus 100 μg LF_{E687A}), LET (100 μg PA plus 100 μg LF_{1-254}-EDIN), LETm (100 μg PA plus 100 μg LF_{1-254}-$EDIN_{R185E}$), or EDIN (1 μg). (A) Six hours following toxin injection mice were inoculated with FITC-dextran (50 μg/mice), and they were euthanized 30 min later for analysis. The images are representative photomicrographs of FITC-dextran (green) diffusion in lung vessels corresponding to a confocal optical section. Anti-CD31 revealed endothelial cells (red). Scale bar, 50 μm. (B and C) Quantitative measurement of pulmonary vessel permeability by diffusion of FITC-dextran in the lung. At the indicated times mice were inoculated with FITC-dextran (50 μg/mouse) 30 min prior to recovery of FITC-dextran in lung as described in Materials and Methods. A.U., arbitrary units. (B) Circles indicate values obtained for individual mice. (C) Pulmonary endothelium permeability determined for eight mice per condition (means ± standard deviations).

death, as previously observed (17, 26). In addition, we show that the chimeric toxin LET induces the formation of large tunnels in endothelial monolayers in a PA-dependent manner. Unlike EDIN alone, LET triggers complete inhibition of RhoA and massive formation of giant transcellular tunnels 4 h after addition of the toxin to endothelial cell monolayers.

LT and LET induced lung vascular permeability. We further investigated the effects of injection of toxin by comparing lung vascular permeabilities in mice intoxicated with either LT or LET. Mice were first intoxicated by intravenous injection of toxins, which was followed by injection of FITC-dextran, using standard techniques (16, 28). The increase in vascular permeability induced by both toxins was shown by direct visualization of the diffusion of FITC-dextran in the vessel walls (Fig. 4A). The effects could be confirmed by quantitative measurement of FITC-dextran extravasation in the lung (Fig. 4B). Neither LE nor LF alone nor catalytically inactive mutants of LT (LTm) and LET (LETm) triggered detectable vascular leakage in lung tissues (data not shown and Fig. 4B). Strikingly, LT triggered a progressive increase in endothelium permeability between 8 and 15 h after toxin injection. At 5 h LET produced an increase in endothelium permeability greater than that produced by LT at 15 h (Fig. 4B). We also found that injection of EDIN alone produced, after 24 h of intoxication, a low and nonlethal level of permeabilization similar to that produced by LT at 8 h (Fig. 4C). Using a smaller dextran (molecular weight, 3,000), we also observed an increase in lung vascular permeability in toxin-treated mice compared to controls, although the differences were not statistically significant (data not shown). Also, this marker was recovered in the urine of all mice, including controls, indicating that this smaller molecule is not suitable for this type of measurement. This is in agreement with previously described permeability measurements obtained under physiological conditions using dextran with a molecular weight of 70,000 because its size is similar to that of serum albumin (2). Importantly, variations in vascular permeabilization between LT and LET directly correlate with the differences in toxin catalytic activities.

In conclusion, here we compared the toxic effects of two structurally related toxins, both of which enter by the PA-dependent import pathway and which differ only by their catalytic domain. LT triggers massive formation of actin cables and an increase in cell death, leading to intercellular junction opening (26). In contrast, LET produces a dramatic disruption of actin cables and formation of transcellular openings in the absence of induction of cell death. Thus, although LT and LET do not trigger direct cell permeabilization, they both induce loss of the endothelium barrier function by corrupting the actin cytoskeleton organization.

Initially, LET was designed as a means to counteract the induction of actin cables by LT and thus rescue its effect on the increase in endothelium permeability. Indeed, treatment of LT-intoxicated cells by LET produced a LET phenotype, but it also led to an increase in endothelium permeability (not shown). Thus, strategies other than direct RhoA inhibition by LET have to be developed to counter the LT effect on endothelium barrier function.

The cytotoxicity of LET is PA dependent and requires

EDIN catalytic activity. Our results thus clearly indicate that the progressive nature of the effect of LT on endothelium permeabilization is related to its activity on MAP kinase kinases. Interestingly, the kinetics of MEK cleavage and previously reported rapid macrophage death contrasts with the late induction of vascular permeability and death due to the toxin in a BALB/c mouse model. In line with this, it has been suggested that a direct effect of LT on the endothelium could play a key role in the induction of vascular permeability and animal death (17, 26). Our results establish that the increase in endothelium permeability due to LT is directly correlated to LT cytotoxicity. This suggests new ways to design therapeutic drugs against anthrax directed toward vascular permeability.

ACKNOWLEDGMENTS

We are grateful to A. Doye, P. Colosetti, and A. Mettouchi for discussions and technical help and to Madhavi Maddugoda for critical reading of the manuscript.

We thank the Conseil Régional PACA and the Conseil Général des Alpes-Maritimes for their financial support of the microscopy facility platform at the C3M Research Center. Our laboratory is supported by institutional funding from INSERM, by a grant and a fellowship to M.R. from the Agence Nationale de la Recherche (grant ANR RPV07055ASA), and by a grant from the Association pour la Recherche sur le Cancer (grant ARC 4906).

REFERENCES

1. **Abrami, L., S. H. Leppla, and F. G. van der Goot.** 2006. Receptor palmitoylation and ubiquitination regulate anthrax toxin endocytosis. J. Cell Biol. **172:**309–320.
2. **Antonetti, D. A., A. J. Barber, S. Khin, E. Lieth, J. M. Tarbell, and T. W. Gardner.** 1998. Vascular permeability in experimental diabetes is associated with reduced endothelial occludin content: vascular endothelial growth factor decreases occludin in retinal endothelial cells. Penn State Retina Research Group. Diabetes **47:**1953–1959.
3. **Arora, N., and S. H. Leppla.** 1994. Fusions of anthrax toxin lethal factor with Shiga toxin and diphtheria toxin enzymatic domains are toxic to mammalian cells. Infect. Immun. **62:**4955–4961.
4. **Barth, H., K. Aktories, M. R. Popoff, and B. G. Stiles.** 2004. Binary bacterial toxins: biochemistry, biology, and applications of common *Clostridium* and *Bacillus* proteins. Microbiol. Mol. Biol. Rev. **68:**373–402.
5. **Bolcome, R. E., III, S. E. Sullivan, R. Zeller, A. P. Barker, R. J. Collier, and J. Chan.** 2008. Anthrax lethal toxin induces cell death-independent permeability in zebrafish vasculature. Proc. Natl. Acad. Sci. USA **105:**2439–2444.
6. **Bonuccelli, G., F. Sotgia, P. G. Frank, T. M. Williams, C. J. de Almeida, H. B. Tanowitz, P. E. Scherer, K. A. Hotchkiss, B. I. Terman, B. Rollman, A. Alileche, J. Brojatsch, and M. P. Lisanti.** 2005. ATR/TEM8 is highly expressed in epithelial cells lining *Bacillus anthracis*' three sites of entry: implications for the pathogenesis of anthrax infection. Am. J. Physiol. Cell Physiol. **288:**C1402–C1410.
7. **Boyer, L., A. Doye, M. Rolando, G. Flatau, P. Munro, P. Gounon, R. Clement, C. Pulcini, M. R. Popoff, A. Mettouchi, L. Landraud, O. Dussurget, and E. Lemichez.** 2006. Induction of transient macroapertures in endothelial cells through RhoA inhibition by *Staphylococcus aureus* factors. J. Cell Biol. **173:**809–819.
8. **Bradley, K. A., J. Mogridge, M. Mourez, R. J. Collier, and J. A. Young.** 2001. Identification of the cellular receptor for anthrax toxin. Nature **414:**225–229.
9. **Carbajal, J. M., and R. C. Schaeffer, Jr.** 1999. RhoA inactivation enhances endothelial barrier function. Am. J. Physiol. **277:**C955–C964.
10. **Collier, R. J., and J. A. Young.** 2003. Anthrax toxin. Annu. Rev. Cell Dev. Biol. **19:**45–70.
11. **Doye, A., L. Boyer, A. Mettouchi, and E. Lemichez.** 2006. Ubiquitin-mediated proteasomal degradation of Rho proteins by the CNF1 toxin. Methods Enzymol. **406:**447–456.
12. **Duesbery, N. S., C. P. Webb, S. H. Leppla, V. M. Gordon, K. R. Klimpel, T. D. Copeland, N. G. Ahn, M. K. Oskarsson, K. Fukasawa, K. D. Paull, and G. F. Vande Woude.** 1998. Proteolytic inactivation of MAP-kinase-kinase by anthrax lethal factor. Science **280:**734–737.
13. **Goletz, T. J., K. R. Klimpel, N. Arora, S. H. Leppla, J. M. Keith, and J. A. Berzofsky.** 1997. Targeting HIV proteins to the major histocompatibility complex class I processing pathway with a novel gp120-anthrax toxin fusion protein. Proc. Natl. Acad. Sci. USA **94:**12059–12064.
14. **Gozes, Y., M. Moayeri, J. F. Wiggins, and S. H. Leppla.** 2006. Anthrax lethal toxin induces ketotifen-sensitive intradermal vascular leakage in certain inbred mice. Infect. Immun. **74:**1266–1272.
15. **Grinberg, L. M., F. A. Abramova, O. V. Yampolskaya, D. H. Walker, and J. H. Smith.** 2001. Quantitative pathology of inhalational anthrax I: quantitative microscopic findings. Mod. Pathol. **14:**482–495.
16. **Guery, B. P., S. Nelson, N. Viget, P. Fialdes, W. R. Summer, E. Dobard, G. Beaucaire, and C. M. Mason.** 1998. Fluorescein-labeled dextran concentration is increased in BAL fluid after ANTU-induced edema in rats. J. Appl. Physiol. **85:**842–848.
17. **Kirby, J. E.** 2004. Anthrax lethal toxin induces human endothelial cell apoptosis. Infect. Immun. **72:**430–439.
18. **Menetrey, J., G. Flatau, E. A. Stura, J. B. Charbonnier, F. Gas, J. M. Teulon, M. H. Le Du, P. Boquet, and A. Menez.** 2002. NAD binding induces conformational changes in Rho ADP-ribosylating *Clostridium botulinum* C3 exoenzyme. J. Biol. Chem. **277:**30950–30957.
19. **Moayeri, M., D. Haines, H. A. Young, and S. H. Leppla.** 2003. *Bacillus anthracis* lethal toxin induces TNF-alpha-independent hypoxia-mediated toxicity in mice. J. Clin. Investig. **112:**670–682.
20. **Moayeri, M., and S. H. Leppla.** 2004. The roles of anthrax toxin in pathogenesis. Curr. Opin. Microbiol. **7:**19–24.
21. **Pezard, C., P. Berche, and M. Mock.** 1991. Contribution of individual toxin components to virulence of *Bacillus anthracis*. Infect. Immun. **59:**3472–3477.
22. **Rmali, K. A., M. A. Al-Rawi, C. Parr, M. C. Puntis, and W. G. Jiang.** 2004. Upregulation of tumour endothelial marker-8 by interleukin-1beta and its impact in IL-1beta induced angiogenesis. Int. J. Mol. Med. **14:**75–80.
23. **Scobie, H. M., G. J. Rainey, K. A. Bradley, and J. A. Young.** 2003. Human capillary morphogenesis protein 2 functions as an anthrax toxin receptor. Proc. Natl. Acad. Sci. USA **100:**5170–5174.
24. **Sharma, M., H. Khanna, N. Arora, and Y. Singh.** 2000. Anthrax toxin-mediated delivery of cholera toxin-A subunit into the cytosol of mammalian cells. Biotechnol. Appl. Biochem. **32:**69–72.
25. **Stearns-Kurosawa, D. J., F. Lupu, F. B. Taylor, Jr., G. Kinasewitz, and S. Kurosawa.** 2006. Sepsis and pathophysiology of anthrax in a nonhuman primate model. Am. J. Pathol. **169:**433–444.
26. **Warfel, J. M., A. D. Steele, and F. D'Agnillo.** 2005. Anthrax lethal toxin induces endothelial barrier dysfunction. Am. J. Pathol. **166:**1871–1881.
27. **Wojciak-Stothard, B., and A. J. Ridley.** 2003. Rho GTPases and the regulation of endothelial permeability. Vasc. Pharmacol. **39:**187–199.
28. **You, D., L. Waeckel, T. G. Ebrahimian, O. Blanc-Brude, P. Foubert, V. Barateau, M. Duriez, S. Lericousse-Roussanne, J. Vilar, E. Dejana, G. Tobelem, B. I. Levy, and J. S. Silvestre.** 2006. Increase in vascular permeability and vasodilation are critical for proangiogenic effects of stem cell therapy. Circulation **114:**328–338.

Editor: S. R. Blanke